Chemical Science

ROYAL SOCIETY OF CHEMISTRY

EDGE ARTICLE

View Article Online
View Journal | View Issue



Cite this: *Chem. Sci.*, 2024, **15**, 5340

All publication charges for this article have been paid for by the Royal Society of Chemistry

Received 30th October 2023
Accepted 8th March 2024

DOI: 10.1039/d3sc05766f

rsc.li/chemical-science

# A pyridinium-based strategy for lysine-selective protein modification and chemoproteomic profiling in live cells†

Chuan Wan,‡[c] Dongyan Yang,‡[d] Chunli Song,[b] Mingchan Liang,[b] Yuhao An,[b] Chenshan Lian,[b] Chuan Dai,[b] Yuxin Ye,[b] Feng Yin,*[b] Rui Wang*[b] and Zigang Li*[ab]

Protein active states are dynamically regulated by various modifications; thus, endogenous protein modification is an important tool for understanding protein functions and networks in complicated biological systems. Here we developed a new pyridinium-based approach to label lysine residues under physiological conditions that is low-toxicity, efficient, and lysine-selective. Furthermore, we performed a large-scale analysis of the ~70% lysine-selective proteome in MCF-7 cells using activity-based protein profiling (ABPP). We quantifically assessed 1216 lysine-labeled peptides in cell lysates and identified 386 modified lysine sites including 43 mitochondrial-localized proteins in live MCF-7 cells. Labeled proteins significantly preferred the mitochondria. This pyridinium-based methodology demonstrates the importance of analyzing endogenous proteins under native conditions and provides a robust chemical strategy utilizing either lysine-selective protein labeling or spatiotemporal profiling in a living system.

## Introduction

Site-selective protein modification under native, complex conditions is useful for both biological and pharmaceutical sciences. A facile and biocompatible method to incorporate synthetic molecules onto proteins could enable direct protein identification, providing information about protein function and structure relevant for disease diagnosis and drug development.[1–5] Several methods have been developed for selective protein labeling in living systems. Among them, genetically encodable strategies using unnatural amino acids have been the most widely used in a live cell environment.[6,7] However, some chemical methods for protein modification are often limited by high toxicity, poor uptake/distribution, and the complicated operation of many conventional methods.[8,9] Creating further complexity, protein functions are regulated by a variety of subcellular compartments within their native habitats. As a result, few chemical methods are suitable for labeling native/endogenous proteins for live cell-based proteomics.[10–14] Ideally, combining site-selective modifications and protein feature profiling would also directly exploit the subcellular organelle compartments in live cells.

Lysine makes up 5.7% of the human proteome, is typically found on protein surfaces (8.9% of surface residues[15]), and is a weak nucleophile at physiological pH,[16,17] making it the third most popular target in the CovPDB database.[18] Although it has great promise, only one FDA approved drug "vigabatrin[17]" targets a lysine site. Thus, generating a broader lysine targeting toolbox is of great interest to current drug discovery.[19,20]

Recently, state-of-art methodologies were developed for lysine-selective modification and active-lysine protein profiling.[21–25] Among them, an activated ester amine transesterification reaction is one of the most practical and robust methodologies (Fig. 1a).[26–28] For example, a sulfotetrafluorophenyl (STP) ester probe was utilized by the Cravatt group for global lysine reactivity and ligandability profiling in the human proteome.[29,30] Each of these activated esters has relative advantages and disadvantages, but a method that enables efficient proteome labeling and profiling in live cells is missing from the current toolbox.[31–33]

To overcome these live system application limitations, we recently investigated using sulfonium probes.[20,34–38] We achieved several successful applications and found that the probes had good aqueous solubility, good cellular uptake, and outstanding nucleophilicity from their positive charge.[39–41] However, sulfonium is a soft acid, making it relatively unstable in the reductive cellular environment.[42] Thus, we envisioned that another positively charged compound and harder acid, quaternary pyridinium, which has been widely used in mitochondria-targeting

[a]*State Key Laboratory of Chemical Oncogenomics, School of Chemical Biology and Biotechnology, Peking University Shenzhen Graduate School, Shenzhen, 518055, P. R. China. E-mail: lizg.sz@pku.edu.cn*

[b]*Pingshan Translational Medicine Center, Shenzhen Bay Laboratory, Shenzhen, 518118, P. R. China. E-mail: yinfeng@szbl.ac.cn; wangrui@szbl.ac.cn; lizg@szbl.ac.cn*

[c]*College of Health Science and Environmental Engineering, Shenzhen Technology University, Shenzhen, 518118, P. R. China*

[d]*College of Chemistry and Chemical Engineering, Zhongkai University of Agriculture and Engineering, Guangzhou, 510225, P. R. China*

† Electronic supplementary information (ESI) available. See DOI: https://doi.org/10.1039/d3sc05766f

‡ These authors contributed equally to this work.

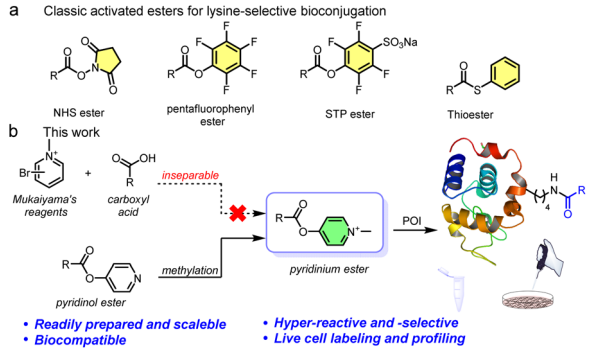


Fig. 1 (a) Examples of classical activated esters for ~70% lysine-selective bioconjugation. (b) Design concept of pyridinium-based lysine-selective modification and profiling.

moieties, would be more applicable to live systems.[43,44] Several excellent bioconjugate methods were previously reported that used pyridinium substrates, including cysteine conjugation[45] and elimination to dehydroalanine (Dha),[46] protein N-terminal amine transamination,[47,48] and photoinduced tryptophan-selective modification in peptides and proteins[49] (see Fig. S1†). Considering this, we expect that the exceedingly electron deficient quaternizated N atom would act as a carboxyl activating group that could be utilized in an efficient amine transesterification reaction for quick, clean, and selective lysine modification. Actually, Mukaiyama's reagent (2-halogenated pyridinium) has been extensively used for amidation and esterification in organic chemistry *via* a 2-acyloxy-*N*-methylpyridinium intermediate,[50] which provides a solid foundation for our proposition. However, direct application of Mukaiyama's reagent would not achieve chemo-selective peptide and protein amidation.[51] Therefore, revisiting pyridinium activated esters is an opportunity to assess a highly reactive methodology together with optimized biophysical properties and mitochondrial enrichment for endogenous protein modification.

Here we report a facile lysine-selective protein modification using a cationic pyridinium activated ester (Fig. 1b). The esters could be readily prepared, were bench stable for months, and had high amino reactivity and a 70% lysine-selective labeling. We then performed activity-based protein profiling (ABPP) for active lysines in cells. In total, we quantitatively identified 350 high-reactive lysine-labeled peptides in 250 proteins in MCF-7 cell lysates. In addition, we achieved labeling 248 proteins containing 386 modified lysine residues in live cells, confirmed by a certain mitochondrial colocalization imaging, suggesting the mitochondrial targeting was due to the positively charged esters.[52] Consequently, pyridinium activated esters provide a promising toolbox to further facilitate spatiotemporal proteome investigation and genetic manipulation.

## Results and discussion

### Design and identification of pyridinium activated esters

We initially examined the direct aromatic nucleophilic substitution ($S_NAr$) of carboxylic acid by Mukaiyama's reagent but obtained complex and inseparable mixtures. Alternately, we tested 4-pyridinol ester **1a** methylation by methyl iodide (MeI) or methyl trifluoromethanesulfonate (MeOTf) and obtained pyridinium pellets with nearly quantitative yields (Fig. 2a). In addition, we established that the pyridinium ester water solubility was around 10 mM, and the pyridinium esters were satisfactorily hydrolysis-resistant in different aqueous solutions (see the preparation of pyridinium activated esters in Fig. S2†). In the metabolic properties of pyridinium ester probes, we performed a hydrolysis assay with carboxylesterase enzyme (using carboxylesterase 1 (CE1) *in vitro* and Chang liver cells (rich in carboxylesterases) in cells). We observed no obvious hydrolysis with carboxylesterase enzyme and found a satisfactorily effective pyridinium ester concentration within live cells (Fig. S2b†). In contrast, 2-pyridinol ester methylation led to a highly unstable pyridinium.

Having successfully synthesized aqueous-stable pyridinium activated esters, we examined the amidation of **1b**, **1c**, and control reagents (pyridinol ester **1a** and NHS ester **1d**) with Boc-Lys-OH *via* $^1$H NMR spectroscopy (in sodium phosphate (NaPi, pH 7.0, in $D_2O$ with 40% $CD_3OD$) solution for 1 hour) (see more esters in Fig. S3†). We added $CD_3OD$ to increase solubility, as substrates other than pyridinium esters are highly hydrophobic. Preliminary activating group screening demonstrated that the pyridinium esters' reactivities were comparable to NHS ester (80–90% yields). Interestingly, we detected a prototropic rearrangement of the leaving enol to the more stable keto form (Fig. S4†), which may provide additional driving force for the transesterification (Fig. 1a).[53] We conducted a detailed kinetic study to gain more insight into the pyridinium esters' reactivities (Fig. 2b and S4†). The results demonstrated that pyridinium esters **1b** and **1c** reacted with lysine significantly faster (observed rate constant $k_{obs} = 0.50\ M^{-1}\ s^{-1}$) than pyridinol ester **1a** ($k_{obs} = 0.16\ M^{-1}\ s^{-1}$) and NHS ester **1d** ($k_{obs} = 0.15\ M^{-1}\ s^{-1}$). Moreover, the excellent efficiency in the aqueous solvent suggested that the pyridinium activated esters would be physiologically compatible.

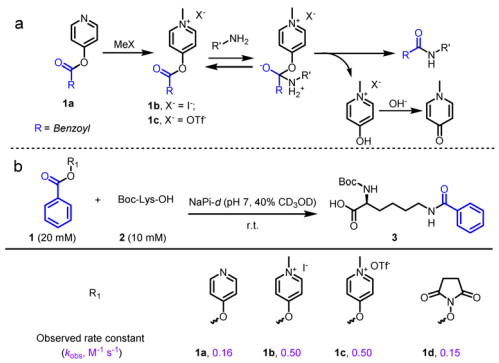


Fig. 2 Developing of pyridinium activated esters enable amidation. (a) Postulated mechanism of amidation with pyridinium esters. (b) Kinetic study between activated esters and Boc-Lys-OH. Conditions: activated ester **1** (20 mM), Boc-Lys-OH **2** (10 mM) in NaPi (pH 7, in $D_2O$ with 40% $CD_3OD$) at room temperature. Two replicates were conducted for the calculation of observed rate constants ($k_2$, $M^{-1}\ s^{-1}$).

We further investigated the pyridinium esters to comprehensively determine their reactivity, solubility, and stability. We conducted peptide and protein amidation to demonstrate the pyridinium esters' reactivity and chemo-selectivity. We prepared lysine (K)-reactive probes (**KP1** and **KP2**, 10 mM), the alkynyl derivatives of **1b** and **1c**, and reacted them with model peptides in PBS (pH 7.4, 50% $CH_3CN$ was added to dissolve peptides) (Fig. 3). Product **4-a**, with dual amidation at the N-terminus and lysine side chain, was observed with 99% conversion after 1 hour of the **KP1**/**KP2** and peptide **4** reaction. Note that we used **KP2** as a substrate for the following reactions due to the iodine anion's potential reducibility. The kinetic study demonstrated that the reaction was finished within 10 min (inset chart in Fig. 3a and Data S1†). To further illustrate their reactivity and chemo-selectivity, we conducted a kinetic comparison between **KP2** and NHS ester **KP11** (Fig. 4) in pH 6.0–8.0 buffers. **KP2** maintained a high reactivity (99% conversion for **4-a**) even at a pH as low as 6.5, but the NHS probe **KP11** could barely complete the reaction (83% conversion for **4-a**) at pH 8.0 after 1 hour (see ESI Tables S1 and S2† for additional data). Interestingly the pyridinium ester exhibited apparent selectivity at the N-terminus in low pH 6.0 buffer. In contrast, the NHS ester only slightly improved the N-terminal reaction selectivity at low pH 6.0 to 6.5. Thus, we performed an in-depth study of the N-terminal-selective peptide and protein modification with pyridinium esters. We found that cyclic peptide **5**, which contains

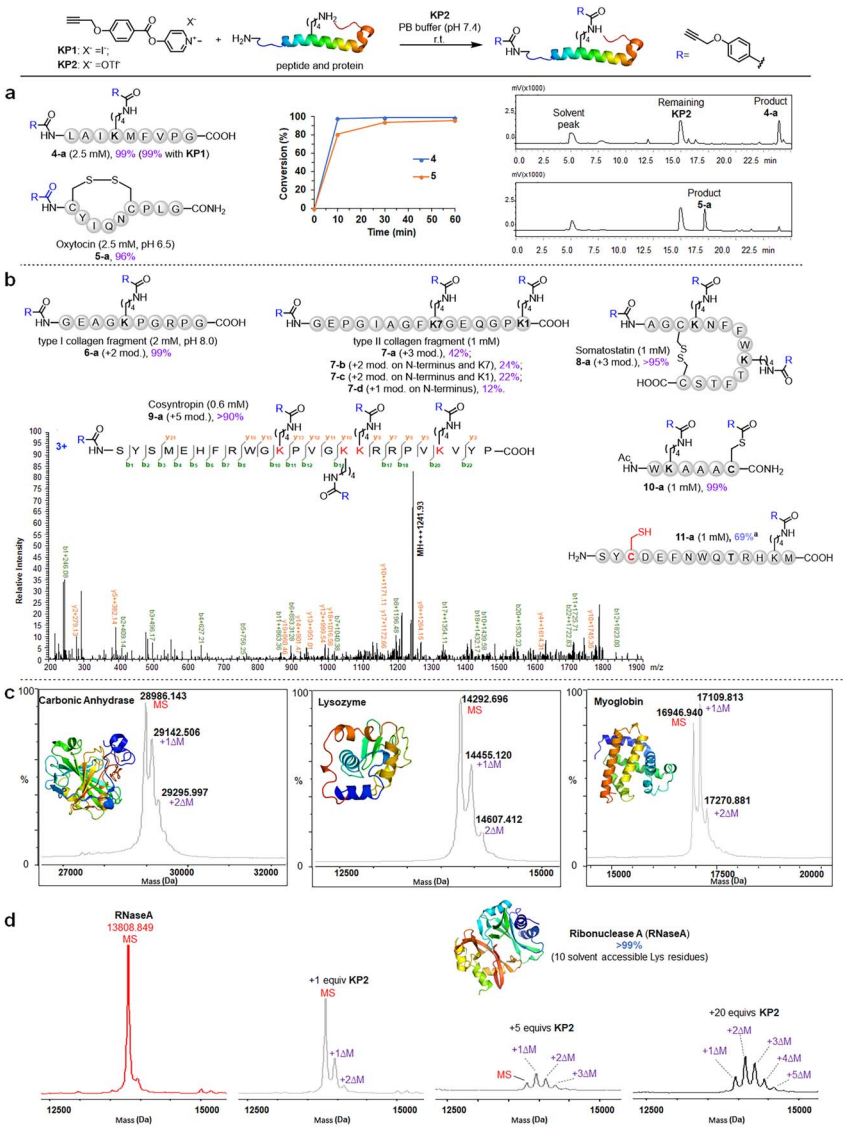


Fig. 3 Chemoselective amidation of pyridinium esters on lysine residue sites in peptides and proteins. (a) Model reactions between **KP2** and peptides, the inserted chart exhibits HPLC determined conversion *versus* time plot, and the LC traces of directly analyzing of reaction mixtures of peptide **4** and **5**. Standard conditions for peptide: **KP2** (10 mM), peptide (indicated concentration in parenthesis) and in PB buffer (pH 7.4, 50% MeCN) for 1 hour at rt. (b) Range of bioactive peptides and protein fragments. "+*n* mod." refers to the number of modifications on the amino groups. (c and d) Modification efficiency of **KP2** on proteins by MALDI-TOF analysis. $\Delta M = 158$ Da. Standard conditions for protein: **KP2** (50 μM, 250 μM and 1000 μM, respectively), protein (50 μM) and in PBS (pH 7.4) for 1 hour at 37 °C. [a] 20 mM DTT was added after amidation.

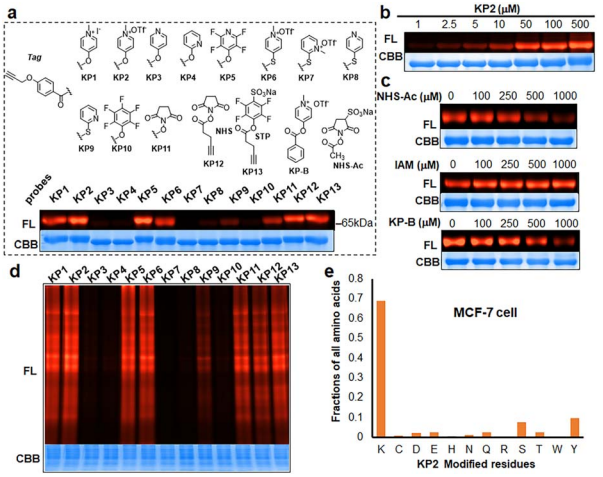


Fig. 4 Qualitative assessment of respective modification performance of probes (**KP1–KP13**). (a) Modification of BSA (10 μg) with **KP1–KP13** (100 μM). (b) Dose-dependent modification of BSA protein with **KP2**. (c) Competitive modification of BSA protein with **KP2** (100 μM) in the increased dose of IAM, NHS-Ac and **KP-B**. (d) Labeling performance of probes in cell lysates. (e) **KP2** preferentially labels lysine residues in MCF-7 cell proteomes. FL, in-gel fluorescence scanning. CBB, Coomassie gel.

only one N-terminal amino group, yielded 96% amidated product **5-a** at pH 6.5, indicating that the pyridinium ester has the potential to be N-terminal-selective in a weakly acidic environment. Moreover, we obtained LC traces by directly analyzing reaction mixtures (Fig. 3a) and found that the reactions typically proceeded with high chemo-selectivity. We also detected the remaining excess **KP2** in the LC traces.

## Pyridinium activated ester probe labels lysine containing proteins

We next moved to more complex bioactive peptides and protein fragments. **KP2** reacted well with all investigated 10-mer to 24-mer peptides (Fig. 3b) that contained a free N-terminal amine and at least one lysine residue. For peptides **6–8** (10–15 amino acid (AA) resides), we conducted the type I and type II collagen fragment (**6** and **7**) and peptide **8** reactions in a different manner. The peptide **6** reaction resulted in 99% conversion of bisamidated product **6-a** at a slightly higher pH (8.0), and we isolated four products from the peptide **7** reaction comprising triple modification (42% of **7-a**), double modification (24% of **7-b**, 22% of **7-c**), and single modification on the N-terminus (12% of **7-d**) at standard conditions (pH 7.4). Note that a trial reaction at pH 8.0 caused significant degradation of peptide **7**. The relatively low reactivity may be due to the helical conformation and multiple exposed carboxyl groups in collagen fragments **6** and **7**, which may cause lysine residue p$K_a$ changes and/or pH changes in the peptide microenvironment. Reacting the cyclic peptide somatostatin **8** (a human hormone analogue) resulted in excellent conversion (>95% for **8-a**) for amine group triple modification at standard conditions. We further demonstrated **KP2**'s reactivity and selectivity during the late stage amidation of a 24 AA-containing peptide. Peptide **9** (cosyntropin, a synthetic adrenocorticotropic hormone) was reacted with **KP2** and resulted in a +5 modification product **9-a** with excellent conversion (>90%). To investigate the chemo-selectivity between amino and thiol groups, we conducted a reaction at standard conditions using lysine and cysteine residue-containing peptide **10**. We found double modification on both **10-a** lysine and cysteine sites, and we observed no other side reactions between the pyridinium salt and cysteine. Additionally, we found that cysteine contributed few side effects in the following profiling studies, which may be attributed to thioesters' instability under physiological conditions. To validate the hypothesis regarding thioester and to conduct a more in-depth exploration of the chemical selectivity of this reaction, we designed a model peptide **11** containing all nucleophilic amino acids. Following the reaction, the addition of dithiothreitol (DTT) facilitated the successful acquisition of the amidation product **11a**, achieving a conversion of 69%. This result further demonstrates the chemical selectivity of the peptide amidation method based on pyridinium ester. We analyzed all peptide products using tandem MS/MS to confirm the reactions' site selectivity (Fig. 3b and ESI†).

We next evaluated the amidation reaction of **KP2** with lysine-containing proteins at high dilution. We used ribonuclease A (RNaseA), carbonic anhydrase (CA), lysozyme, and myoglobin as model proteins, and we conducted equimolar reactions between model proteins (50 μM) and **KP2** (50 μM) under physiological conditions (PBS, pH 7.4, 37 °C for 1 hour). We analyzed the resulting **KP2**-labeled protein products using MALDI-TOF (Fig. 3c). We clearly observed one or two modifications for all four proteins at this dilute concentration. Furthermore, we found that the RNaseA amidation was **KP2** dose-dependent over concentrations ranging from 0 to 1 mM (Fig. 3d). We increased the conversions by increasing ester equivalents. With 20 equiv. of **KP2**, we observed quantitative conversion with one to five amidated modifications. Collectively, we revealed that peptide and protein amidation reactions with pyridinium esters had high reactivity and chemo-selectivity, suggesting a potential pyridinium-based tool to be further validated for protein labeling and profiling in more complex systems.

We next prepared a series of alkyne-tagged ester probes (**KP1–KP13**), including pyridinium esters and control reagents (Fig. 4a), and utilized them to investigate bovine serum albumin (BSA) labeling profiles after copper-catalyzed azide alkyne cycloaddition (CuAAC) coupling with a fluorescent dye (TAMRA-$PEG_3$-$N_3$). We incubated the probes (100 μM) with BSA under physiological conditions (PBS, pH 7.4, 37 °C for 1 hour) and found that **KP2** performed comparable well. Furthermore, the reaction between **KP2** and BSA proceeded in a dose-dependent manner (Fig. 4b). We also performed competition reactions using lysine- and cysteine-reactive reagents and found that excess NHS-Ac pretreatment decreased the fluorescence intensity, but iodoacetamide (IAM) pretreatment had negligible influence (Fig. 4c), indicating that **KP2** predominantly labeled BSA protein lysine residues but not cysteine residues. We further confirmed this using LC-MS/MS (ESI Table S3†). We

consistently found weaker fluorescence intensity after pretreatment with excess pyridinium ester competitor (**KP-B**).

### *In vitro* labeling lysine residues containing proteome

Inspired by pyridinium ester's high protein-labeling efficiency, we next evaluated the human proteome lysine reactivity profile. We first established the **KP1–KP13** (100 μM, room temperature (RT) for 1 hour) labeling profiles in MCF-7 cell lysates using in-gel fluorescence scanning. Similar labeling intensity was observed for 100 μM **KP2** compared to 100 μM of **KP11** and **KP12** (NHS esters), and **KP13** (STP) (Fig. 4d). Also, **KP2** labeling appeared to be dose-dependent and time-dependent (Fig. S5a and b†). In a competitive labeling experiment, the fluorescent bands became weaker after pretreatment with NHS-Ac or competitor (**KP-B**) but not IAM, suggesting that **KP2** labeled proteins in a lysine-/KP-specific manner (Fig. S5c of in-gel fluorescence imaging and Fig. S7c of cellular imaging in cells†). Next we incorporated **KP2**-labeled fragments into photolytic tags (PC-biotin-$N_3$) to enrich for the labeled MCF-7 cell lysate proteome using streptavidin beads. The photo-released labeled peptides were then analysed using LC-MS/MS. The hydroxyl-containing AAs tyrosine (9.5%) and serine (8.3%) were partially labeled, and the majority of **KP2**-labeled sites were lysine residues (67.9% on average) (Fig. 4e and ESI Table S4†), highlighting a certain lysine-selectivity of pyridinium esters comparing with the NHS and STP esters (Fig. S6†). To visualize the statistical significance of the frequency of modified-lysines containing peptides (Tables S4 and S5d†), we further performed a pLogo[54] analysis to show the **KP2** labeling pattern. Argine (R), glycine (G) and alaine (A) residues were significantly enriched at −1/+3/−6 positions around lysines, respectively. Next, we quantitatively assessed the active lysine residues labeled by **KP2** using tandem orthogonal proteolysis-activity-based protein profiling (TOP-ABPP) with label-free quantification (LFQ) without normalization (see ESI†) when a large-scale change in the global modification occurs.[55] We prepared two pairwise **KP2** concentrations (10 : 10 μM and 100 : 10 μM) in two parallel experiments with MCF-7 cells (Fig. 5a and ESI Table S5†). Highly reactive lysines (387 **KP2**-labeled peptides) could be enriched with low-concentration **KP2**, yielding nearly equivalent intensities as that of high-dose **KP2** ($0 < R_{100:10} \leq 2$) (Fig. 5b). The **KP2**-labeled peptide spectra that met our quality control confidence criteria with quantified values in all samples were selected for analysis. The 350 potential high-reactive lysine-labeled peptides (at both ratios of $0.67 \leq R_{10:10} \leq 1.5$ and $0 < R_{100:10} \leq 2.0$) in 250 proteins that spanned protein classes, including kinases, chaperones, and structural proteins (Fig. 5c).

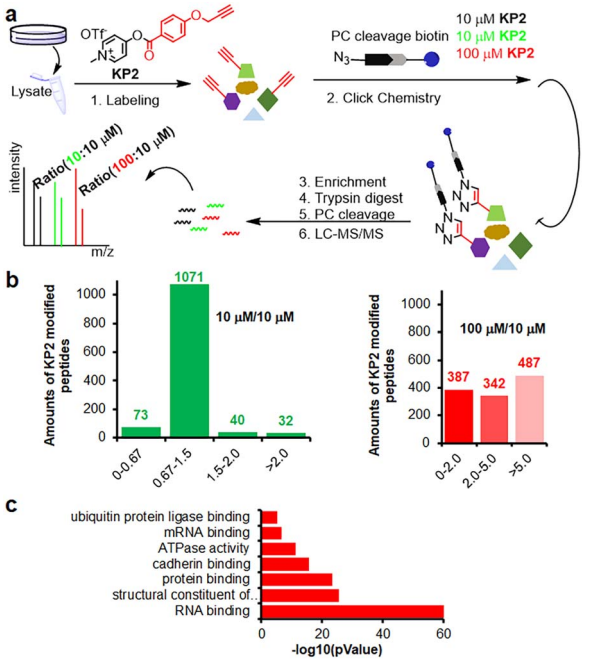


Fig. 5 Chemoproteomic lysine profiling with **KP2** in MCF-7 cells. (a) The workflow of tandem orthogonal proteolysis-activity-based protein profiling (TOP-ABPP) combined with label-free quantification. (b) Identified LFQ TOP-ABPP ratios for peptides from MCF-7 cells labeled with two **KP2** concentrations (100 : 10 μM in red color) and (10 : 10 μM in green color) (ESI Table S5†). (c) MF (molecular function) analysis for 350 high-reactive lysine containing proteins (at both ratios of $0.67 \leq R_{10:10} \leq 1.5$ and $0 < R_{100:10} \leq 2.0$).

### Mitochondrial-labeled proteome profiling in live cells

We next evaluated **KP2** biocompatibility in live cells. We measured $IC_{50}$ values in MCF-7 cells and found that 500 μM **KP2** showed almost no toxicity, much less than NHS and STP esters (Fig. 6a and S7a†). To perform an *in situ* labeling of **KP2**, we first used in-gel fluorescent signals to preliminarily optimize the labeling conditions. Notably, cell culture medium ingredients consume **KP2**; thus, it was necessary to conduct the live cell labeling in PBS buffer for 1 hour. As additionally shown in Fig. 6b, labeling proteins with 500 μM **KP2** in cells yielded the lowest signals but no toxicity to MCF-7 live cells. The cellular imaging was then performed to assess **KP2** labeling[56] (Fig. 6c and S7b†), in which 2.5 μM **KP2** was incubated in live MCF-7/HeLa cells for 1 hour, then fixed and permeabilized, followed by TAMRA-$N_3$ click. It is noteworthy that a lower concentration of 2.5 μM **KP2** was utilized in the cell imaging assays to mitigate the detrimental effects of excessive fluorescence probe on imaging outcomes. Since macrophage inflammatory responses are important during immune responses,[57] we also applied **KP2** labeling to RAW264.7 macrophages. Interestingly, we discovered that **KP2** appeared to be a partially mitochondrial location, possibly because of its positive charge. Therefore, we examined **KP2** labeling colocalization with two mitochondrial markers in live MCF-7/HeLa/RAW264.7 cells, heat shock protein 60 (HSP60, blue) and cytochrome c oxidase subunit 4 isoform 1 (COX4, green) (Fig. 6d and S7b†).

Finally, based on above optimized conditions (Fig. 6a and b), we used 500 μM **KP2** to label MCF-7 live cell in culture dish replaced with PBS buffer for one hour to successfully collect 386 modified lysine sites in 248 proteins (ESI Table S6†). Distinguishable **KP2**-labeled proteins were further explored and systematically compared (Fig. 6e). These proteins showed a diverse cellular components (CC) as annotated in the GO database.[58] CC analysis in live cells revealed 43 unique proteins

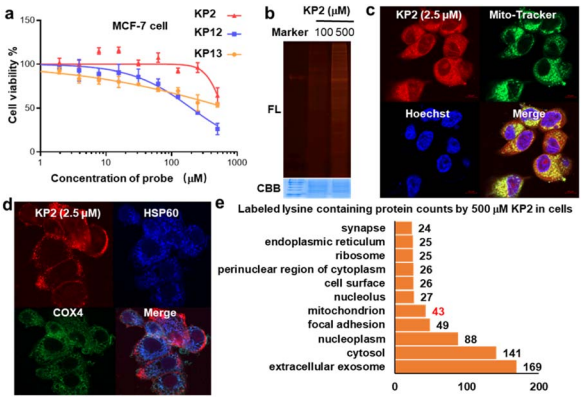


Fig. 6 *In situ* profiling human proteome by **KP2**. (a) $IC_{50}$ values of the probes (**KP2**, **KP12**, **KP13**) against MCF-7 cell. Data represent means ± standard deviation for three experiments. (b) **KP2** probe labeling proteins in MCF-7 live cells, by ABPP in-gel fluorescence scanning and CBB, treated with **KP2** probe 1 hour followed conjugation of TAMRA-$N_3$ by CuAAC click-chemistry. FL, in-gel. (c) Cellular imaging of **KP2** (2.5 μM) with live MCF-7 cells. **KP2** exhibited the strongest *in situ* labeling in live MCF-7 cells after 1 hour of treatment, colocalized with that of MitoTracker green FM. Scale bar = 10 μm. Correlation was determined by Manders overlap coefficient (MOC = 0.94529). (d) Immunofluorescent analysis of MCF-7 live cells after **KP2** labeling validated the labeled mitochondria proteins. The colocalization of TAMRA immunofluorescence (red) conjugated by **KP2** with two mitochondrial markers cytochrome *c* oxidase subunit 4 isoform 1 (COX4, green) and Heat Shock Protein 60 (HSP60, blue). Scale bar = 10 μm. (e) Cellular component (CC) analysis for **KP2** labeled lysines containing proteins labeled by 500 μM **KP2**.

in mitochondrion, consistent with our findings in imaging. Taken together, we revealed that to a certain extent pyridinium-based **KP2** labeling was lysine-selective and mitochondria-labeling. Thus, **KP2** can potentially be used to detect endogenous lysine-specific sites both *in vitro* and in live cells. In the future, it would be valuable to derive more pyridinium-based strategies for spatiotemporal changes in living systems.

## Conclusions

Here we developed a cationic pyridinium activated ester to label and profile active lysine proteins. The pyridinium ester exhibited effective lysine reactivity and ~70% selectivity. We applied **KP2** to human proteome ABPP and quantitatively identified 350 high-reactive lysine-labeled peptides by LFQ. Remarkably, we also used **KP2** for lysine-selective proteome profiling in live cells and identified 386 lysine sites in 248 proteins. To the best of our knowledge, this is a rare, successful case of lysine selective ABPP in a complex system. Additionally, the cationic pyridinium ester demonstrated the potential for mitochondrial-localized labeling in live cells. In future, we will continue to improve **KP2**'s lysine selectivity, organelle-specificity, and metabolic features. In conclusion, we developed a pyridinium-based activated ester with good reactivity, a ~70% lysine selectivity, and biocompatibility that provides a complimentary alternative for lysine-selective modification and organelle-targeted chemoproteomic profiling.

## Data availability

Materials, protocols, and data characterizations for all chemical and biological experiments are provided in the ESI.† Protein lists from mass spectrometry identification (XLSX), proteomics data have been deposited to the ProteomeXchange Consortium (http://proteomecentral.proteomexchange.org) *via* the iProX partner repository[59] with the project ID IPX0004016001. The data that support the findings of this study are available.

## Author contributions

Research was conceived by FY, RW and ZL. Experiments were designed by CW, FY and ZL. Chemical experiments were conducted by CW and CD. Biochemical assays and chemoproteomic experiments were performed by DY, CS, ML, CL, XY, YA and RW. The manuscript was written and proofread by all authors.

## Conflicts of interest

The authors declare no competing financial interest.

## Acknowledgements

We acknowledge financial support from the National Key Research and Development Program "Synthetic Biology" Key Special Project of China, 2021YFC2103902 and 2021YFA0910803; Natural Science Foundation of China grants 22307081, 32302420, 22307084, 21977010, 21977011 and 22107045; the Guangdong Basic and Applied Basic Research Foundation, 2022A1515010996; the Shenzhen Science and Technology Program, JCYJ20230807151059004, JCYJ20220818095808019, RCJC20200714114433053, JCYJ20180508152213145 5, JCYJ20200109140406047 and JCYJ20180507182427559; Tian Fu Jin Cheng Laboratory (Advanced Medical Center) Group Racing Project, TFJC2023010008; Science and Technology Program in Guangzhou 202102020214; the Shenzhen People's Hospital funds SYKYPY201909. We acknowledge financial support from Shenzhen-Hong Kong Institute of Brain Science-Shenzhen Fundamental Research Institutions (2023SHIBS0004). Shenzhen High-tech Zone Development Special Plan Pingshan District Innovation Platform Construction Project (29853MKCJ202300208). Technical support from the Mass Spectrometry Core Facility of Shenzhen Bay Laboratory and Dr Fan Yang of Peking University are gratefully acknowledged.

## Notes and references

1 T. Tamura and I. Hamachi, Chemistry for Covalent Modification of Endogenous/Native Proteins: From Test Tubes to Complex Biological Systems, *J. Am. Chem. Soc.*, 2019, **141**, 2782–2799.
2 E. A. Hoyt, P. M. S. D. Cal, B. L. Oliveira and G. J. L. Bernardes, Contemporary approaches to site-

selective protein modification, *Nat. Rev. Chem*, 2019, **3**, 147–171.
3 O. Koniev and A. Wagner, Developments and recent advancements in the field of endogenous amino acid selective bond forming reactions for bioconjugation, *Chem. Soc. Rev.*, 2015, **44**, 5495–5551.
4 C. G. Parker and M. R. Pratt, Click Chemistry in Proteomic Investigations, *Cell*, 2020, **180**, 605–632.
5 C. Kwak, C. Park, M. Ko, C. Y. Im, H. Moon, Y. H. Park, S. Y. Kim, S. Lee, M. G. Kang, H. J. Kwon, E. Hong, J. K. Seo and H. W. Rhee, Identification of proteomic landscape of drug-binding proteins in live cells by proximity-dependent target ID, *Cell Chem. Biol.*, 2022, **29**(12), 1739–1753.
6 Y. Ge, X. Fan and P. R. Chen, A genetically encoded multifunctional unnatural amino acid for versatile protein manipulations in living cells, *Chem. Sci.*, 2016, **7**, 7055–7060.
7 R. Zhu, G. Zhang, M. Jing, Y. Han, J. Li, J. Zhao, Y. Li and P. R. Chen, Genetically encoded formaldehyde sensors inspired by a protein intra-helical crosslinking reaction, *Nat. Commun.*, 2021, **12**, 581.
8 A. E. Speers and B. F. Cravatt, Chemical strategies for activity-based proteomics, *Chembiochem*, 2004, **5**, 41–47.
9 E. M. Sletten and C. R. Bertozzi, Bioorthogonal chemistry: fishing for selectivity in a sea of functionality, *Angew Chem. Int. Ed. Engl.*, 2009, **48**, 6974–6998.
10 K. M. Backus, B. E. Correia, K. M. Lum, S. Forli, B. D. Horning, G. E. Gonzalez-Paez, S. Chatterjee, B. R. Lanning, J. R. Teijaro, A. J. Olson, D. W. Wolan and B. F. Cravatt, Proteome-wide covalent ligand discovery in native biological systems, *Nature*, 2016, **534**, 570–574.
11 C. G. Parker, A. Galmozzi, Y. Wang, B. E. Correia, K. Sasaki, C. M. Joslyn, A. S. Kim, C. L. Cavallaro, R. M. Lawrence, S. R. Johnson, I. Narvaiza, E. Saez and B. F. Cravatt, Ligand and Target Discovery by Fragment-Based Screening in Human Cells, *Cell*, 2017, **168**, 527–541.
12 A. E. Speers, G. C. Adam and B. F. Cravatt, Activity-based protein profiling in vivo using a copper(i)-catalyzed azide-alkyne [3 + 2] cycloaddition, *J. Am. Chem. Soc.*, 2003, **125**, 4686–4687.
13 R. M. Reja, W. Wang, Y. Lyu, F. Haeffner and J. Gao, Lysine-Targeting Reversible Covalent Inhibitors with Long Residence Time, *J. Am. Chem. Soc.*, 2022, **144**, 1152–1157.
14 M. Tan, J. Ma, X. Yang, Q. You, X. Guo, Y. Li, R. Wang, G. Han, Y. Chen, X. Qiu, X. Wang and L. Zhang, Quantitative proteomics reveals differential immunoglobulin-associated proteome (IgAP) in patients of acute myocardial infarction and chronic coronary syndromes, *J. Proteomics*, 2022, **252**, 104449.
15 F. Tekaia, E. Yeramian and B. Dujon, Amino acid composition of genomes, lifestyles of organisms, and evolutionary trends: a global picture with correspondence analysis, *Gene*, 2002, **297**, 51–60.
16 G. Platzer, M. Okon and L. P. McIntosh, pH-dependent random coil (1)H, (13)C, and (15)N chemical shifts of the ionizable amino acids: a guide for protein pK a measurements, *J. Biomol. NMR*, 2014, **60**, 109–129.
17 J. W. Wheless, R. E. Ramsay and S. D. Collins, Vigabatrin, *Neurotherapeutics*, 2007, **4**, 163–172.
18 M. Gao, A. F. A. Moumbock, A. Qaseem, Q. Xu and S. Gunther, CovPDB: a high-resolution coverage of the covalent protein-ligand interactome, *Nucleic Acids Res.*, 2022, **50**, D445–D450.
19 J. Ha, H. Park, J. Park and S. B. Park, Recent advances in identifying protein targets in drug discovery, *Cell Chem. Biol.*, 2021, **28**, 394–423.
20 Y. Xie, S. Du, Z. Liu, M. Liu, Z. Xu, X. Wang, J. X. Kee, F. Yi, H. Sun and S. Q. Yao, Chemical Biology Tools for Protein Lysine Acylation, *Angew Chem. Int. Ed. Engl.*, 2022, **61**, e202200303.
21 S. R. Adusumalli, D. G. Rawale, K. Thakur, L. Purushottam, N. C. Reddy, N. Kalra, S. Shukla and V. Rai, Chemoselective and Site-Selective Lysine-Directed Lysine Modification Enables Single-Site Labeling of Native Proteins, *Angew. Chem.*, 2020, **132**, 10418–10422.
22 T. Tamura, T. Ueda, T. Goto, T. Tsukidate, Y. Shapira, Y. Nishikawa, A. Fujisawa and I. Hamachi, Rapid labelling and covalent inhibition of intracellular native proteins using ligand-directed N-acyl-N-alkyl sulfonamide, *Nat. Commun.*, 2018, **9**, 1870.
23 M. J. Matos, B. L. Oliveira, N. Martinez-Saez, A. Guerreiro, P. Cal, J. Bertoldo, M. Maneiro, E. Perkins, J. Howard, M. J. Deery, J. M. Chalker, F. Corzana, G. Jimenez-Oses and G. J. L. Bernardes, Chemo- and Regioselective Lysine Modification on Native Proteins, *J. Am. Chem. Soc.*, 2018, **140**, 4004–4017.
24 D. A. Shannon, R. Banerjee, E. R. Webster, D. W. Bak, C. Wang and E. Weerapana, Investigating the proteome reactivity and selectivity of aryl halides, *J. Am. Chem. Soc.*, 2014, **136**, 3330–3333.
25 P. M. Cal, J. B. Vicente, E. Pires, A. V. Coelho, L. F. Veiros, C. Cordeiro and P. M. Gois, Iminoboronates: a new strategy for reversible protein modification, *J. Am. Chem. Soc.*, 2012, **134**, 10299–10305.
26 Y. Yasueda, T. Tamura, A. Fujisawa, K. Kuwata, S. Tsukiji, S. Kiyonaka and I. Hamachi, A Set of Organelle-Localizable Reactive Molecules for Mitochondrial Chemical Proteomics in Living Cells and Brain Tissues, *J. Am. Chem. Soc.*, 2016, **138**, 7592–7602.
27 M. E. Abbasov, M. E. Kavanagh, T. A. Ichu, M. R. Lazear, Y. Tao, V. M. Crowley, C. W. Am Ende, S. M. Hacker, J. Ho, M. M. Dix, R. Suciu, M. M. Hayward, L. L. Kiessling and B. F. Cravatt, A proteome-wide atlas of lysine-reactive chemistry, *Nat. Chem.*, 2021, **13**, 1081–1092.
28 S. Choi, S. Connelly, N. Reixach, I. A. Wilson and J. W. Kelly, Chemoselective small molecules that covalently modify one lysine in a non-enzyme protein in plasma, *Nat. Chem. Biol.*, 2010, **6**, 133–139.
29 S. M. Hacker, K. M. Backus, M. R. Lazear, S. Forli, B. E. Correia and B. F. Cravatt, Global profiling of lysine reactivity and ligandability in the human proteome, *Nat. Chem.*, 2017, **9**, 1181–1190.
30 M. E. Abbasov, M. E. Kavanagh, T. A. Ichu, M. R. Lazear, Y. Tao, V. M. Crowley, C. W. Am Ende, S. M. Hacker, J. Ho,

M. M. Dix, R. Suciu, M. M. Hayward, L. L. Kiessling and B. F. Cravatt, A proteome-wide atlas of lysine-reactive chemistry, *Nat. Chem.*, 2021, **13**, 1081–1092.

31 J. A. Prescher and C. R. Bertozzi, Chemistry in living systems, *Nat. Chem. Biol.*, 2005, **1**, 13–21.

32 D. L. Fortin, M. R. Banghart, T. W. Dunn, K. Borges, D. A. Wagenaar, Q. Gaudry, M. H. Karakossian, T. S. Otis, W. B. Kristan, D. Trauner and R. H. Kramer, Photochemical control of endogenous ion channels and cellular excitability, *Nat. Methods*, 2008, **5**, 331–338.

33 Z. Huang, Z. Liu, X. Xie, R. Zeng, Z. Chen, L. Kong, X. Fan and P. R. Chen, Bioorthogonal Photocatalytic Decaging-Enabled Mitochondrial Proteomics, *J. Am. Chem. Soc.*, 2021, **143**, 18714–18720.

34 D. Wang, M. Yu, N. Liu, C. Lian, Z. Hou, R. Wang, R. Zhao, W. Li, Y. Jiang, X. Shi, S. Li, F. Yin and Z. Li, A sulfonium tethered peptide ligand rapidly and selectively modifies protein cysteine in vicinity, *Chem. Sci.*, 2019, **10**, 4966–4972.

35 A. D. Guo, D. Wei, H. J. Nie, H. Hu, C. Peng, S. T. Li, K. N. Yan, B. S. Zhou, L. Feng, C. Fang, M. Tan, R. Huang and X. H. Chen, Light-induced primary amines and o-nitrobenzyl alcohols cyclization as a versatile photoclick reaction for modular conjugation, *Nat. Commun.*, 2020, **11**, 5472–5485.

36 R. Griffiths, F. R. Smith, J. E. Long, H. Williams, R. Layfield and N. Mitchell, Site-Selective Modification of Peptides and Proteins via Interception of Free Radical-Mediated Dechalcogenation, *Angew Chem. Int. Ed. Engl.*, 2020, **59**(52), 23659–23667.

37 Z. Hou, Y. Wang, C. Wan, L. Song, R. Wang, X. Guo, D. Yang, Y. Zhang, X. Qin, Z. Zhou, X. Zhang, F. Yin and Z. Li, Sulfonium Triggered Alkyne-Azide Click Cycloaddition, *Org. Lett.*, 2022, **24**, 1448–1453.

38 C. Wan, Y. Zhang, J. Wang, Y. Xing, D. Yang, Q. Luo, J. Liu, Y. Ye, Z. Liu, F. Yin, R. Wang and Z. Li, Traceless Peptide and Protein Modification via Rational Tuning of Pyridiniums, *J. Am. Chem. Soc.*, 2024, **146**(4), 2624–2633.

39 X. Shi, R. Zhao, Y. Jiang, H. Zhao, Y. Tian, Y. Jiang, J. Li, W. Qin, F. Yin and Z. Li, Reversible stapling of unprotected peptides via chemoselective methionine bis-alkylation/dealkylation, *Chem. Sci.*, 2018, **9**, 3227–3232.

40 W. Li, D. Wang, X. Shi, J. Li, Y. Ma, Y. Wang, T. Li, J. Zhang, R. Zhao, Z. Yu, F. Yin and Z. Li, A siRNA-induced peptide co-assembly system as a peptide-based siRNA nanocarrier for cancer therapy, *Mater. Horiz.*, 2018, **5**, 745–752.

41 Y. Y. Li, X. J. Wang, Y. L. Su, Q. Wang, S. W. Huang, Z. F. Pan, Y. P. Chen, J. J. Liang, M. L. Zhang, X. Q. Xie, Z. Y. Wu, J. Y. Chen, L. Zhou and X. Luo, Baicalein ameliorates ulcerative colitis by improving intestinal epithelial barrier via AhR/IL-22 pathway in ILC3s, *Acta Pharmacol. Sin.*, 2022, **43**, 1495–1507.

42 T.-L. Ho, Hard soft acids bases (HSAB) principle and organic chemistry, *Chem. Rev.*, 1975, **75**, 1–20.

43 Y. Huang, G. Zhang, R. Zhao and D. Zhang, Aggregation-Induced Emission Luminogens for Mitochondria-Targeted Cancer Therapy, *ChemMedChem*, 2020, **15**, 2220–2227.

44 M. Tian, J. Zhan and W. Lin, Single fluorescent probes enabling simultaneous visualization of duple organelles: Design principles, mechanisms, and applications, *Coord. Chem. Rev.*, 2022, **451**, 214266.

45 M. J. Matos, C. D. Navo, T. Hakala, X. Ferhati, A. Guerreiro, D. Hartmann, B. Bernardim, K. L. Saar, I. Companon, F. Corzana, T. P. J. Knowles, G. Jimenez-Oses and G. J. L. Bernardes, Quaternization of Vinyl/Alkynyl Pyridine Enables Ultrafast Cysteine-Selective Protein Modification and Charge Modulation, *Angew Chem. Int. Ed. Engl.*, 2019, **58**, 6640–6644.

46 J. M. Chalker, S. B. Gunnoo, O. Boutureira, S. C. Gerstberger, M. Fernández-González, G. J. L. Bernardes, L. Griffin, H. Hailu, C. J. Schofield and B. G. Davis, Methods for converting cysteine to dehydroalanine on peptides and proteins, *Chem. Sci.*, 2011, **2**, 1666.

47 L. S. Witus, C. Netirojjanakul, K. S. Palla, E. M. Muehl, C. H. Weng, A. T. Iavarone and M. B. Francis, Site-specific protein transamination using N-methylpyridinium-4-carboxaldehyde, *J. Am. Chem. Soc.*, 2013, **135**, 17223–17229.

48 K. S. Palla, L. S. Witus, K. J. Mackenzie, C. Netirojjanakul and M. B. Francis, Optimization and expansion of a site-selective N-methylpyridinium-4-carboxaldehyde-mediated transamination for bacterially expressed proteins, *J. Am. Chem. Soc.*, 2015, **137**, 1123–1129.

49 S. J. Tower, W. J. Hetcher, T. E. Myers, N. J. Kuehl and M. T. Taylor, Selective Modification of Tryptophan Residues in Peptides and Proteins Using a Biomimetic Electron Transfer Process, *J. Am. Chem. Soc.*, 2020, **142**, 9112–9118.

50 T. Mukaiyama, New Synthetic Reactions Based on the Onium Salts of Aza-Arenes [New synthetic methods (29)], *Angew Chem. Int. Ed. Engl.*, 1979, **18**, 707–721.

51 D. Crich and I. Sharma, Epimerization-free block synthesis of peptides from thioacids and amines with the Sanger and Mukaiyama reagents, *Angew Chem. Int. Ed. Engl.*, 2009, **48**, 2355–2358.

52 F. N. Vogtle, J. M. Burkhart, H. Gonczarowska-Jorge, C. Kucukkose, A. A. Taskin, D. Kopczynski, R. Ahrends, D. Mossmann, A. Sickmann, R. P. Zahedi and C. Meisinger, Landscape of submitochondrial protein distribution, *Nat. Commun.*, 2017, **8**, 290.

53 Z. J. Kaminski, B. Kolesinska, J. Kolesinska, G. Sabatino, M. Chelli, P. Rovero, M. Blaszczyk, M. L. Glowka and A. M. Papini, N-triazinylammonium tetrafluoroborates. A new generation of efficient coupling reagents useful for peptide synthesis, *J. Am. Chem. Soc.*, 2005, **127**, 16912–16920.

54 J. P. O'Shea, M. F. Chou, S. A. Quader, J. K. Ryan, G. M. Church and D. Schwartz, pLogo: a probabilistic approach to visualizing sequence motifs, *Nat. Methods*, 2013, **10**, 1211–1212.

55 O. Kauko, T. D. Laajala, M. Jumppanen, P. Hintsanen, V. Suni, P. Haapaniemi, G. Corthals, T. Aittokallio, J. Westermarck and S. Y. Imanishi, Label-free quantitative phosphoproteomics with novel pairwise abundance normalization reveals synergistic RAS and CIP2A signaling, *Sci. Rep.*, 2015, **5**, 13099.

56 D. Zhu, H. Guo, Y. Chang, Y. Ni, L. Li, Z.-M. Zhang, P. Hao, Y. Xu, K. Ding and Z. Li, Cell- and Tissue-Based Proteome Profiling and Dual Imaging of Apoptosis Markers with Probes Derived from Venetoclax and Idasanutlin, *Angew. Chem., Int. Ed.*, 2018, **57**, 9284–9289.
57 R. Medzhitov, Origin and physiological roles of inflammation, *Nature*, 2008, **454**, 428–435.
58 D. N. Itzhak, S. Tyanova, J. Cox and G. H. Borner, Global, quantitative and dynamic mapping of protein subcellular localization, *Elife*, 2016, **5**, e16950.
59 J. Ma, T. Chen, S. Wu, C. Yang, M. Bai, K. Shu, K. Li, G. Zhang, Z. Jin, F. He, H. Hermjakob and Y. Zhu, iProX: an integrated proteome resource, *Nucleic Acids Res.*, 2019, **47**, D1211–D1217.